

Magnon and Hole Excitations in the Two-Dimensional Half-filled Hubbard Model

Weihong Zheng¹, Rajiv R. P. Singh², Jaan Oitmaa¹, Oleg P. Sushkov¹ Chris J. Hamer¹

¹*School of Physics, University of New South Wales,
Sydney, NSW 2052, Australia*

²*Department of Physics,
University of California, Davis, CA 95616*

(Dated: November 13, 2018)

Spin and hole excitation spectra and spectral weights are calculated for the half-filled Hubbard model, as a function of t/U . We find that the high energy spin spectra are sensitive to charge fluctuations. The energy difference $\Delta(\pi, 0) - \Delta(\pi/2, \pi/2)$, which is negative for the Heisenberg model, changes sign at a fairly small $t/U \approx 0.053(5)$. The hole bandwidth is proportional to J , and considerably larger than in the t - J models. It has a minimum at $(\pi/2, \pi/2)$ and a very weak dispersion along the antiferromagnetic zone boundary. A good fit to the measured spin spectra in La_2CuO_4 at $T = 10\text{K}$ is obtained with the parameter values $U = 3.1\text{eV}$, $t = 0.35\text{eV}$.

PACS numbers: 75.10.Jm

I. INTRODUCTION

Underdoped phases of high temperature superconducting materials and the nature of the metal insulator transition upon doping a Mott-insulating antiferromagnet remain central topics of research in condensed matter physics. Some puzzles extend all the way to the undoped stoichiometric insulating materials. Results such as the antiferromagnetic zone-boundary magnon excitations probed in inelastic neutron scattering^{1,2}, the two-magnon excitations probed in Raman scattering³ and the one-hole excitations probed in angle-resolved photoemission spectroscopy⁴ continue to surprise us. The question of whether some of these anomalies are connected to the pseudogap phase of the weakly doped materials remains a topic of debate.

An important question is the extent to which conventional approaches, based on ordered antiferromagnetic phases, can explain the observed spectra and spectral weights and to what extent the interpretation of data necessitates the introduction of novel ideas such as spin-liquids and spin-charge separation. The low energy long-wavelength spin excitations of the antiferromagnet are well described by the non-linear sigma model⁵. However, the high energy zone-boundary spin excitations necessarily require a microscopic lattice model. The antiferromagnetic insulator, without charge fluctuations, is represented by the Heisenberg model, and the excitation spectrum of this model has been the subject of several controlled numerical studies^{6,7,8}. It is clear that the antiferromagnetic zone-boundary spectrum of La_2CuO_4 does not agree with that of the Heisenberg model. In particular, in the Heisenberg model, the magnon energy difference $\Delta(\pi, 0) - \Delta(\pi/2, \pi/2)$ is negative but it is found to be positive for La_2CuO_4 . This result will be worse if second neighbor antiferromagnetic interactions are included. It has been suggested that one way to reconcile the difference is by invoking ring-exchange terms^{1,2,9,10}, which arise due to charge fluctuations¹¹.

Here, we present systematic numerical calculations of the magnon and hole spectra and spectral weights of the Hubbard model as a function of t/U . First, we focus on the magnons. Earlier the magnon spectra were studied by mean-field theory¹² and by a Quantum Monte Carlo Simulation combined with the Single Mode Approximation¹³, neither of which are expected to be quantitatively accurate for small t/U . Our calculations show that the zone-boundary magnon energies are very sensitive to charge fluctuations and the difference $\Delta(\pi, 0) - \Delta(\pi/2, \pi/2)$ changes sign at a relatively small t/U value of 0.053(5). The magnon spectra of La_2CuO_4 and the spectral weights are well described by the Hubbard model as discussed below.

The calculated hole spectra, on the other hand, are qualitatively similar to previous theoretical studies of Hubbard and t - J models^{14,15}. The hole-bandwidth is suppressed at large U by a factor of t/U , although we find it to still be much larger than in the corresponding t - J models. The minimum is at $(\pi/2, \pi/2)$ with a weak dispersion along the antiferromagnetic zone boundary. Hence, these results cannot be used to fit the observed ARPES spectra in the undoped cuprate materials⁴. Although same-sublattice hopping terms can allow better fits to the dispersion, the anomalous spectral weights remain harder to explain⁴. We note that a complete understanding of the ARPES experiments may require a multi-band model, as well as inclusion of dielectric and charging effects.

To carry out an Ising type expansion^{16,17} for this system at $T = 0$ we consider the Hubbard-Ising model with the following Hamiltonian:

$$\begin{aligned} H &= H_0 + \lambda H_1 \\ H_0 &= J/4 \sum_{\langle ij \rangle} (\sigma_i^z \sigma_j^z + 1) + \sum_{\mathbf{i}} [U(n_{i\uparrow} - \frac{1}{2})(n_{i\downarrow} - \frac{1}{2}) \\ &\quad + h(-1)^{\mathbf{i}} \sigma_{\mathbf{i}}^z] \\ H_1 &= - \sum_{\langle ij \rangle} [J(\sigma_i^z \sigma_j^z + 1)/4 + t(c_{i\sigma}^\dagger c_{j\sigma} + \text{h.c.})] \end{aligned}$$

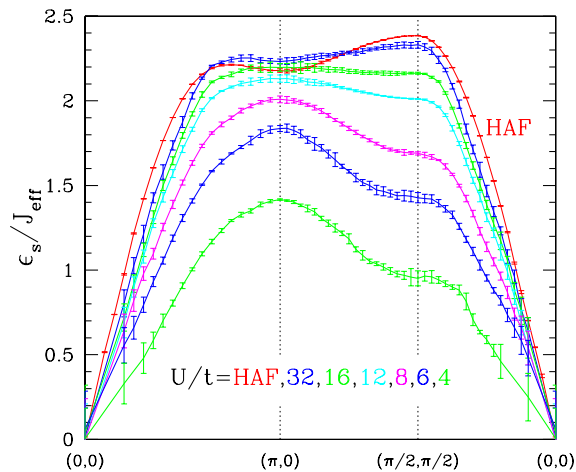


FIG. 1: (Color online) Magnon dispersion curve along selected directions in the Brillouin zone for various values of U/t , expressed in units of $J_{\text{eff}} = 4t^2/U$. Results for the Heisenberg antiferromagnet are shown as a red curve.

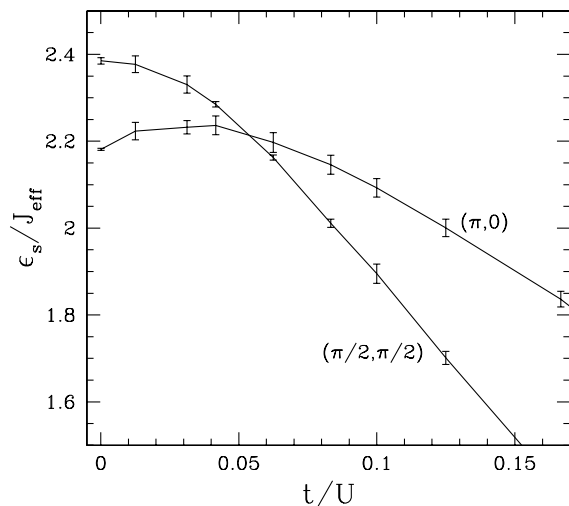


FIG. 2: Magnon energies at two wavevectors along the anti-ferromagnetic zone boundary as a function of t/U .

$$-h \sum_{\mathbf{i}} (-1)^{\mathbf{i}} \sigma_{\mathbf{i}}^z$$

where $\sigma_{\mathbf{i}}^z = n_{\mathbf{i}\uparrow} - n_{\mathbf{i}\downarrow}$, and λ is the expansion parameter. The Ising interaction J is, in principle, an adjustable parameter but here is chosen to be $4t^2/U$. The strength of the staggered field h can be varied to improve convergence. Note that the full Hubbard model is recovered at $\lambda = 1$, at which point the extra terms cancel between H_0 and H_1 . On the other hand for $\lambda < 1$, there is an Ising-like anisotropy in the system, which favors a Néel state and induces a gap in the spectrum. The limit $\lambda = 0$ corresponds to the Ising model, with the usual Néel states being the two unperturbed ground states.

We have extended the linked cluster method¹⁶ to the spectra of the Hubbard-Ising models. At $\lambda = 0$, the model has a very simple excitation spectrum. Above the two ground states, all single spin-flip states (or all states with a single hole for the hole spectra) are degenerate with each other. We construct an orthogonality transformation, which order by order in powers of λ , decouples these single spin-flip states from the rest of the Hilbert space. This procedure amounts to finding the combination of one-flip states with others that remains an eigenstate as λ changes from zero. For a translationally invariant system the resulting block diagonal Hamiltonian in the one particle subspace is diagonalized by Fourier transformation.

To set the normalizations for our calculations, we begin with the definition for the dynamic structure factor

$$S^{\alpha\beta}(\mathbf{q}, \omega) = \frac{1}{2\pi N} \sum_{i,j} \int_{-\infty}^{\infty} \exp[i(\omega t + \mathbf{q} \cdot (\mathbf{r}_i - \mathbf{r}_j))] \langle S_j^\alpha(t) S_i^\beta(0) \rangle dt \quad (1)$$

We define the single magnon contribution to the dynamical transverse structure factor as

$$S^{XX}(\mathbf{q}, \omega) + S^{YY}(\mathbf{q}, \omega) = A_s \delta(\omega - \epsilon_s(\mathbf{q})) + B_s(\mathbf{q}, \omega) \quad (2)$$

Here, $\epsilon_s(\mathbf{q})$ gives the dispersion for the magnons and $A_s(\mathbf{q})$ defines the weights for the magnons. The quantity $B_s(\mathbf{q}, \omega)$ defines the multiparticle contributions. Series expansions have been calculated for the spectra $\epsilon_s(\mathbf{q})$ and the spectral weights $A_s(\mathbf{q})$ up to order λ^{11} .

Similarly, for the hole-excitations, we define the spectral function

$$A(\mathbf{q}, \omega) = \frac{1}{2\pi N} \sum_{i,j} \int_{-\infty}^{\infty} \exp[i(\omega t + \mathbf{q} \cdot (\mathbf{r}_i - \mathbf{r}_j))] \langle c_{j,\sigma}^\dagger(t) c_{i,\sigma}(0) \rangle dt \quad (3)$$

We define the single hole contribution to the spectral function as

$$A(\mathbf{q}, \omega) = A_h \delta(\omega - \epsilon_h(\mathbf{q})) + B_h(\mathbf{q}, \omega) \quad (4)$$

Series expansions are calculated for the hole spectra $\epsilon_h(\mathbf{q})$ and the spectral weights $A_h(\mathbf{q})$ up to order λ^{11} .

The gap in the spectrum closes at $\lambda = 1$, when spin rotational symmetry is restored in the model. This causes power-law singularities in certain properties of the model¹⁸. Hence, the $\lambda = 1$ limit needs to be dealt with by series extrapolation methods. We use the method of integrated differential approximants, well known from the study of critical phenomena¹⁹, to calculate various properties at $\lambda = 1$.

In Figure 1, we show the calculated magnon dispersion, in units of $J_{\text{eff}} = 4t^2/U$, along selected directions in the Brillouin zone, for several values of t/U . The results⁸ for the Heisenberg model are also shown. While the long wavelength spin-wave velocity is gradually reduced with

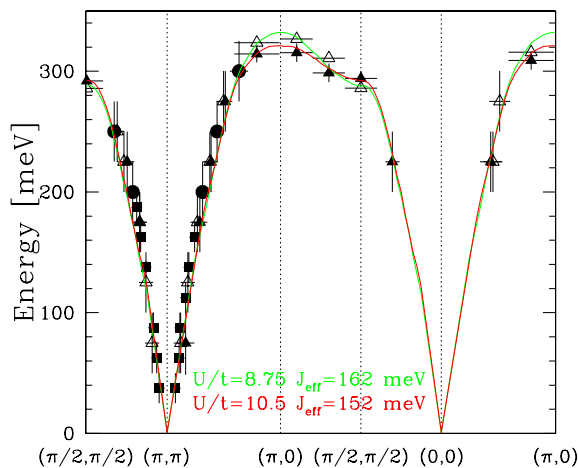


FIG. 3: (Color online) Fits to the spectra of the material La_2CuO_4 : experimental spectra at 10K (open symbols) fit by $U/t = 8.75 \pm 0.7$, $J_{\text{eff}} = 162 \pm 3 \text{ meV}$ (green curve); experimental spectra at 295K (solid symbols) fit with $U/t = 10.5 \pm 0.7$, $J_{\text{eff}} = 152 \pm 3 \text{ meV}$ (red curve).

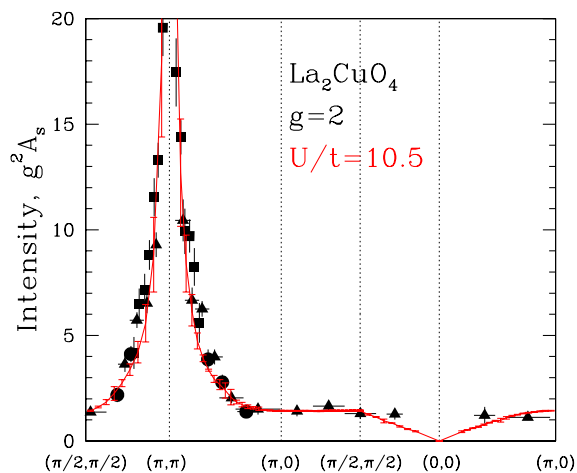


FIG. 4: (Color online) Comparison of magnon spectral weight $g^2 A_s$ for $U/t = 10.5$ with neutron scattering intensity¹ for La_2CuO_4 at 295K.

increasing t/U , other dramatic changes arise along the antiferromagnetic zone boundary. The magnon energy at wavevector $(\pi, 0)$ at first rises briefly before it begins to decrease with increasing t/U . On the other hand, the magnon energy at $(\pi/2, \pi/2)$ decreases sharply with increasing t/U . Both of these are plotted in Figure 2, where one can see that they cross at a relatively small value of $t/U = 0.053(5)$.

In Figures 3 and 4 we show fits to the magnon spectra and spectral weight of La_2CuO_4 . Since we have not done any finite temperature calculations, we try to fit the spectra at different temperatures by effective U and t values. We find that the spectrum at 10K is fitted well

by $U/t = 8.75 \pm 0.7$ and $J_{\text{eff}} = 162 \pm 3 \text{ meV}$, while that at 295K is fitted best by $U/t = 10.5 \pm 0.7$ and $J_{\text{eff}} = 152 \pm 3 \text{ meV}$. These results suggest that as the temperature is increased the effective exchange constant decreases whereas the effective U/t ratio increases. Assuming that the 10K data are essentially at $T = 0$, we obtain bare parameters of $U = 3.1 \text{ eV}$ and $t = 0.35 \text{ eV}$.

The spectral weights are only measured at 295K, hence we show a fit to the calculated spectral weights at the larger U/t ratio. In any case, the spectral weights are not very sensitive to the U/t ratio. The relative fit is excellent. To get a measure of the absolute fit, we first note that the integrated one-magnon spectral weight over the entire zone was²⁰ found from experiment to be 0.36 ± 0.09 , in the normalization where total transverse spectral weight is 0.5. With this normalization, our more accurate calculations for the Heisenberg model give an integrated transverse one-magnon spectral weight of 0.419(2). The one-magnon spectral weights decrease slightly with decreasing U/t , and are also much less accurate, giving 0.40(8) for $U/t = 10$. Hence, the results agree with experiments well within the uncertainties. We should note, however, that this agreement is very much dominated by the $1/q$ dependent behavior near the antiferromagnetic wavevector (where q is the deviation from the antiferromagnetic wavevector), which does not depend much on the microscopic model. The best place to look for multimagnon excitations and a more sensitive comparison with microscopic models is the spectral weight along the antiferromagnetic zone boundary. For the Heisenberg model, the multiparticle spectral weight is largest at $(\pi, 0)$, where it is about 40 percent of the total transverse spectral weight. We hope our work may motivate more accurate measurements of multiparticle spectral weights along the antiferromagnetic zone boundary.

The data on two other systems of square-lattice antiferromagnets $(\text{CuDCOO})_2 \cdot 4\text{D}_2\text{O}$ (CFTD)²¹ and $\text{Cu}(\text{II})$ spins of $\text{Sr}_2\text{Cu}_3\text{O}_4\text{Cl}_2$ ²² have much larger U/t ratios and are well fitted by the Heisenberg model. Allowing U to vary, $(\text{CuDCOO})_2 \cdot 4\text{D}_2\text{O}$ (CFTD) can be well fitted by the Hubbard model with $U/t = 50$ and $U = 3.9 \text{ eV}$. On the other hand, the experimental data on $\text{Sr}_2\text{Cu}_3\text{O}_4\text{Cl}_2$ have substantial uncertainties and anisotropies, so one can not get a reliable estimate for U/t . If one assumes the U value for it is about 4eV, one estimates $U/t \approx 40$.

In Figure 5, we show the single hole excitation spectra along selected directions in momentum space at different values of t/U . Plots are also shown for the t - J model²³, with comparable t/J values. It is evident that the band-width scales with J but is much larger than in the t - J model. The reason for this is the effective same-sublattice hopping generated in the Hubbard model in the order t^2/U which is not included in the t - J model. In all cases, the minimum of the hole energy remains at $(\pi/2, \pi/2)$ and the dispersion along the line $(\pi/2, \pi/2)$ to $(\pi, 0)$ remains weak. As mentioned above, this is in contrast to the observed single hole dispersion⁴ in the material $\text{Sr}_2\text{CuO}_2\text{Cl}_2$. Furthermore, our calculated spec-

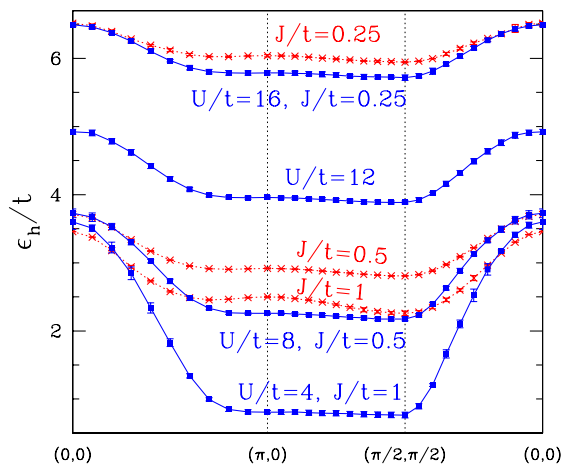


FIG. 5: (Color online) Single hole dispersion in the square-lattice half-filled Hubbard model along selected directions in momentum space for several values of t/U (squares). Also shown as crosses is the dispersion for the t - J model with comparable t/J_{eff} ratios.

tral weights at $(\pi/2, \pi/2)$ and $(\pi, 0)$ are very similar. It has been argued that even small same-sublattice hopping terms can significantly change the shape of the dispersion curves and bring them closer to those observed in ARPES measurements⁴, they may also help reconcile the measured spectral weights in the undoped cuprates²⁴.

In conclusion, we find that allowing for charge fluctuations by making t/U finite allows us to understand the antiferromagnetic zone-boundary excitations in the material La_2CuO_4 very well. However, it appears that the simple one-band Hubbard model considered here is unable to explain the single hole spectra in the undoped cuprate materials.

We would like to thank R. Coldea for useful discussion and sending us the experimental data. This work is supported by the Australian Research Council and the US National Science Foundation grant number DMR-0240918 (RRPS). We are grateful for the computing resources provided by the Australian Partnership for Advanced Computing (APAC) National Facility and by the Australian Centre for Advanced Computing and Communications (AC3).

¹ R. Coldea, *et al.*, Phys. Rev. Lett. **86**, 5377(2001).

² A. A. Katanin and A. P. Kampf, Phys. Rev. B **66**, 100403 (2002).

³ R. R. P. Singh *et al.* Phys. Rev. Lett. **62**, 2736 (1989); B. S. Shastry and B. I. Shraiman, Phys. Rev. Lett. **65**, 1068 (1990); D. K. Morr and A. V. Chubukov, Phys. Rev. B **56**, 9134 (1997); A. A. Katanin and A. P. Kampf, Phys. Rev. B **67**, 100404 (2003).

⁴ A. Damascelli, Z. Hussain and Z.X. Shen, Rev. Mod. Phys. **75**, 473 (2003), and references therein.

⁵ S. Chakravarty, B. I. Halperin and D. R. Nelson, Phys. Rev. B **39**, 2344 (1989).

⁶ A. W. Sandvik and R. R. P. Singh, Phys. Rev. Lett. **86**, 528 (2001).

⁷ R. R. P. Singh and M. P. Gelfand, Phys. Rev. B **52**, 15695 (1995).

⁸ W. Zheng, J. Oitmaa and C.J. Hamer, cond-mat/0412184.

⁹ A. Laeuchli *et al.*, Cond-mat/0412035.

¹⁰ M. Roger, J. H. Hethrington and J. M. Dellerieu, Rev. Mod. Phys. **55**, 1 (1983).

¹¹ A. H. MacDonald, S. M. Girvin and D. Yoshioka, Phys. Rev. B **37**, 9753 (1988). M. Takahashi, J. Phys. C **10**, 1289 (1977).

¹² N. M. R. Peres and M. A. N. Araujo, Phys. Rev. B **65**, 132404 (2002); A. Singh and P. Goswami, Phys. Rev. B **66**, 092402 (2002).

¹³ P. Sengupta, R. T. Scalettar and R. R. P. Singh, Phys. Rev. B **66**, 144420 (2002).

¹⁴ E. Dagotto, Rev. Mod. Phys. **66**, 763 (1994).

¹⁵ N. Bulut, D. J. Scalapino and S. R. White, Phys. Rev. Lett. **73**, 748 (1994).

¹⁶ M.P. Gelfand and R.R.P. Singh, Adv. Phys. **49**, 93(2000).

¹⁷ Z.P. Shi and R.R.P. Singh, Phys. Rev. B **52**, 9620 (1995).

¹⁸ D. A. Huse, Phys. Rev. B **37**, 2380 (1988).

¹⁹ A.J. Guttmann, in "Phase Transitions and Critical Phenomena", Vol. **13** ed. C. Domb and J. Lebowitz (New York, Academic, 1989).

²⁰ R. Coldea, private communication.

²¹ H.M. Ronnow, *et al.* Phys. Rev. Lett. **87**, 037202 (2001).

²² Y.J. Kim, *et al.*, Phys. Rev. B **64**, 024435 (2001).

²³ C. J. Hamer, Zheng Weihong, and J. Oitmaa, Phys. Rev. B **58**, (1998) 15508.

²⁴ O.P. Sushkov, G.A. Sawatzky, R. Eder, and H. Eskes, Phys. Rev. B **56**, 11769 (1997).